



**HAL**  
open science

# A Contrario Oil Tank Detection with Patch Match Completion

Antoine Tadros, Sebastien Drouyer, Rafael Grompone von Gioi

► **To cite this version:**

Antoine Tadros, Sebastien Drouyer, Rafael Grompone von Gioi. A Contrario Oil Tank Detection with Patch Match Completion. IGARSS 2021 - 2021 IEEE International Geoscience and Remote Sensing Symposium, Jul 2021, Brussels, Belgium. pp.4900-4903, 10.1109/IGARSS47720.2021.9553048 . hal-03895616

**HAL Id: hal-03895616**

**<https://hal.science/hal-03895616>**

Submitted on 13 Dec 2022

**HAL** is a multi-disciplinary open access archive for the deposit and dissemination of scientific research documents, whether they are published or not. The documents may come from teaching and research institutions in France or abroad, or from public or private research centers.

L'archive ouverte pluridisciplinaire **HAL**, est destinée au dépôt et à la diffusion de documents scientifiques de niveau recherche, publiés ou non, émanant des établissements d'enseignement et de recherche français ou étrangers, des laboratoires publics ou privés.

# A CONTRARIO OIL TANK DETECTION WITH PATCH MATCH COMPLETION

Antoine Tadros      Sébastien Drouyer      Rafael Grompone von Gioi,

Centre Borelli, ENS Paris-Saclay, CNRS, Université Paris-Saclay, France

## ABSTRACT

The energy sector is a key industry in the global economy and monitoring oil storage provides valuable insights into the economic state of a country. Our aim is to detect oil tank farms as accurately as possible using Sentinel-2 images. An *a contrario* clustering method is used to group by density the result of a circle detection step. Then, a patch-match procedure is used to complete the tank detection. Although most existing methods are designed to work on high-resolution images, the proposed method is designed for low-resolution images; we also propose an adaptation to high-resolution images.

**Index Terms**— Remote Sensing, oil tank, *a contrario* method, circle detection, clustering, patch matching, multi-scale.

## 1. INTRODUCTION

Several methods exist in the literature for oil tank detection in satellite images. Han et al. [1] introduced a geometrical and graph-based method to detect oil tanks and oil tank farms. Based on the method in [1], Cai et al. [2] used an alternative saliency map in combination with the Hough Circle Transform (HCT) and finally trained an SVM to classify the detected circles as oil tanks or not. Jing et al. [3] exhibited and compared several saliency maps for oil tank detection. More recent detectors also use machine learning algorithms to learn features on which a classifier is trained to detect the tanks. The authors of [4, 5, 6] use SURF, HOG, or pretrained neural networks as feature extractors. However, most of the aforementioned methods are designed for high-resolution images which implies a high cost. Instead, we chose to turn to Sentinel-2 images which are free, but with a resolution of only 10 m per pixel.

In [7] an *a contrario* method to detect oil tank farms was presented. It consists of a pipeline in which circles are first detected to identify tank candidates in the image and are then filtered via an *a contrario* clustering method. The *a contrario* framework allows to evaluate how likely an event is to happen

in a noise model which is considered as the null hypothesis  $H_0$ . The less likely an event is under  $H_0$ , the more meaningful it is. The framework introduces the measure of Number of False Alarms (NFA) which is used to evaluate the meaningfulness of an event under  $H_0$ . In this paper we use an *a contrario* patch-match method, developed by Grompone et al. [8], to complete the detection of [7], improving its originally low recall while maintaining its high precision. We also show how to apply the circle detection in a multi-scale fashion to extend the method to high-resolution images and apply it to PlanetScope images.



Fig. 1: Example of site with an oil tank farm.

## 2. A CONTRARIO CLUSTERING

This section provides a brief summary of the oil tank detection pipeline described in [7]; we refer the reader to the original publication for more details.

### 2.1. Circle Detection

The first step computes a sub-pixel edge map using Canny-Devernay’s method [9]. The algorithm provides a list of chained edge points. Only the closed chains are kept, i.e. the chains where the first edge point is linked to the last one. The isoperimetric ratio of the polygon chain is then evaluated. Here, the sub-pixel accuracy is particularly important when working with small targets such as oil tanks in Sentinel-2 images, which appear as circles of radii ranging from 2 to 10 pixels. Closed curves with isoperimetric ratio above  $\rho_{th}$  are classified as circles and, therefore, as oil tank candidates.

Work partly financed by Office of Naval Research grant N00014-17-1-2552 and N00014-20-S-B001, DGA Astrid project filmer la Terre n° ANR-17-ASTR-0013-01 and Kayrros Inc. We thank Carlo de Franchis (Kayrros) and Jean-Michel Morel (ENS Paris-Saclay) for valuable suggestions. We also thank Planet for providing us the PlanetScope images under the Personal Research License.

## 2.2. Generation of meaningful clusters

Once the preliminary circle detection is done, we want to regroup all the detected tanks into clusters based on their proximity. To this end, the method uses binary dilation with a disk pattern to regroup the nearby detected circles. Different sizes of binary dilation are used and all the clusters thus created are kept. A set of overlapping clusters, the clusters candidates, is obtained.

Most of the clusters are irrelevant or may contain the same set of circles. A measure of the relevance, the meaningfulness, is assigned to each cluster candidate.

The *a contrario* framework [10] provides such a measure and provides a way to exclude erroneous detections. The goal of the framework is to exclude irrelevant detections, given a background model  $H_0$ , also called noise model. If a detection is likely to happen under the noise model  $H_0$  it is said to be accidental and is considered to be a false detection.

Let  $N$  be the number of tank candidates in the image. In [7] the background model  $H_0$  is the hypothesis that the positions of the  $N$  circles are drawn uniformly on the image domain and independently from one another. The image domain has its area normalized for the computation.

Under this setting, the probability of having  $k$  circles in a cluster of area  $\sigma$  in the normalized image domain is

$$P_\sigma(k) = \mathcal{B}(N, k, \sigma) = \sum_{i=k}^N \binom{N}{i} \sigma^i (1-\sigma)^{N-i}, \quad (1)$$

where  $\mathcal{B}(N, k, \sigma)$  is the binomial tail. This allows to compute the fundamental quantity in the *a contrario* approach, the NFA, which corresponds to the expected number of occurrence of the event “ $k$  circles are inside a cluster of area  $\sigma$ ” under  $H_0$ :

$$\text{NFA}(k, \sigma) = N_{test} \cdot P_\sigma(k), \quad (2)$$

where  $N_{test}$  is the number of tested position across the image. The NFA score is computed for each cluster candidate, and the ones with  $\text{NFA} < \epsilon$  are kept as detections. The tolerance  $\epsilon$  is set by the operator and corresponds to the average number of false detection allowed per image.

## 2.3. The exclusion principle

The evaluation of the NFA helps to eliminate the cluster with a low density of tank candidates, which are the least relevant. But among the remaining clusters there is often some overlapping. We want to keep only the most meaningful ones. To this end, an exclusion principle presented in [7] is used. Its philosophy is to iteratively keep the cluster of best NFA and reevaluate the meaningfulness of the other clusters, ignoring the circles belonging to the kept cluster. The method is repeated until no meaningful cluster is available.

## 3. COMPLETION BY PATCH SIMILARITY

While the pipeline described in the previous section [7] manages to give a good level of precision, the recall was not satisfactory due to a considerable number of tanks missing at the circle detection step. Missing tanks usually appear with low contrast or with a shadow that breaks the circular shape. In this section, we propose to use an *a contrario* patch match method [8] to complete the detection.

Since the method in Section 2 detects tanks with a high precision, we can randomly extract  $m_p$  patches, centered on the identified tanks, and consider those patches as good references for what is being looked for in the rest of the image. In fact, the tank patches in the image are highly redundant, making a self-similarity algorithm a good fit to complete the tank detection.

### 3.1. A Contrario Patch-Matching

Let  $Q_r$  and  $Q_c$  be respectively a reference patch and a candidate patch, both of size  $N_Q$ . We want to decide if those two patches are similar or not. Knowing that we are looking for patches with some geometric structure, a method based on the gradient orientation comparison seems well suited. In [8], the authors proposed an *a contrario* patch-match method based on the computation of an angular error between the patches’ gradient orientation.

We compute the distance between the patches as

$$d(Q_r, Q_c) = \sum_{i=1}^{N_Q} \frac{|Angle(Q_{r,i}, Q_{c,i})|}{\pi}, \quad (3)$$

where  $Angle(Q_{r,i}, Q_{c,i})$  is the angle error between the  $i^{th}$  element of the patches gradient orientation, given on  $[-\pi, \pi]$ .

We consider the background model  $H'_0$  where the normalized angular error between the gradient orientation of two pixels is considered as drawn from a uniform distribution on  $[0, 1]$ . Under  $H'_0$ , the distance between two patches  $D_{H'_0}$  is then a sum of *i.i.d.* random variables following the uniform distribution. As explained in [8], such a sum of uniform random variables follows the Irwin-Hall distribution:

$$P(D_{H'_0} \leq d) = \frac{1}{N_Q!} \sum_{i=0}^{\lfloor d \rfloor} (-1)^i \binom{N_Q}{i} (d-i)^{N_Q}, \quad (4)$$

where  $\lfloor d \rfloor$  is the integer part of  $d$ . The first term of Eq. (4) is an upper-bound and it was shown in [8] that it provides a good approximation for its value at a much lower computational cost. Thus, the probability of observing a distance  $d$  between two patches is approximated by the relation:

$$P(D_{H'_0} \leq d) \leq \frac{d^{N_Q}}{N_Q!}. \quad (5)$$

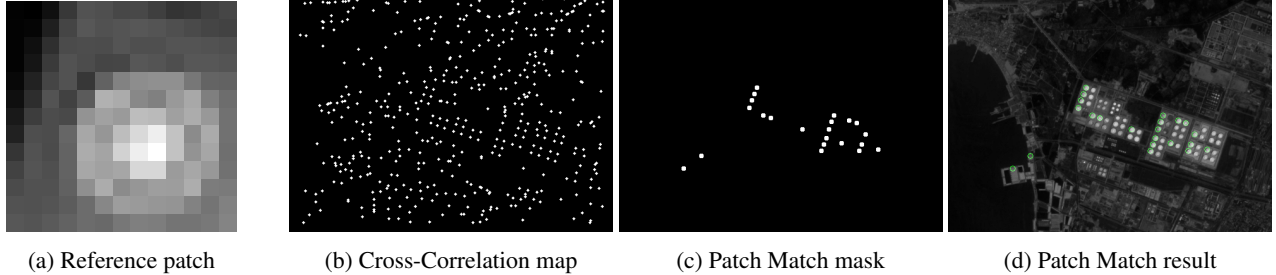


**Fig. 2:** Patch match result with selection of candidate patches via the Cross-Correlation map. The parameter  $\tau$  is set to 0.5.

We define  $NFA_{patch}$  as

$$NFA_{patch}(Q_r, Q_c) = N_T \frac{[d(Q_r, Q_c)]^{N_Q}}{N_Q!}, \quad (6)$$

where  $N_T = N_I^{5/2}$  is the number of tests with  $N_I$  the number of pixels in the image. This is because, in principle, the reference patch can be centered in any pixel ( $N_I$ ), the candidate patch also can be centered in any pixel ( $N_I$ ), and about  $\sqrt{N_I}$  patch sizes are considered. Patches  $Q_c$  and  $Q_r$  are said to match when  $NFA_{patch}(Q_r, Q_c) < \epsilon'$ . We set  $\epsilon' = 1$  which can be interpreted as allowing 1 accidental patch match in the image. We refer the reader to [8] for more details.

### 3.2. Cross-correlation map

To reduce the number of patches to evaluate in practice, we compute the cross-correlation map  $M$  using the method from [11]. The selected candidate patches  $Q_c$  are the patches centered around the local maxima of  $M$ . To further reduce the number of patches to test, we limit the minimum level of correlation allowed for the local maxima with a threshold  $\tau \times \max_M$ , where  $\tau \in [0, 1]$  and  $\max_M$  is the maximum value of cross-correlation. The size of the patches to consider is  $N_Q = (3r)^2$ , where  $r$  is the radius of the circle in the reference patch  $Q_r$ .

If  $NFA_{patch}(Q_r, Q_c) < 1$ , a circle of radius  $r$  is drawn around the center of the patch and is considered to be a new tank candidate. Those new detected circles are added to the list of circles of the valid cluster provided by the method in section 2. Figure 2 illustrates the process of candidate patch selection and patch-matching verification. To avoid getting overlapping detections, new circles are ignored if their center falls inside an already existing circle. In the end, a new detection mask of tank candidates is obtained, on which can be re-applied the *a contrario* clustering method to remove false detections.

### 3.3. Multi-scale circle detection

The aforementioned method in Section 2 is designed for Sentinel-2 image resolution. But what about high-resolution satellite images?

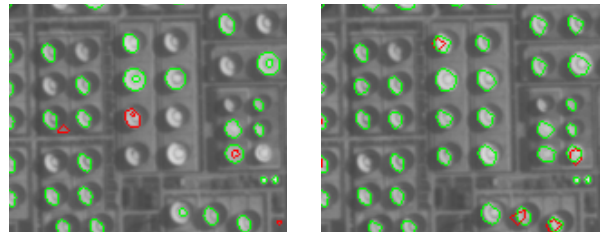


**Fig. 3:** Comparison of single scale and multi-scale circle detection on a PlanetScope image. The shapes in green are those which are classified as circles by isoperimetric thresholding ( $\rho_{th} = 0.9$ ), in red are those which have been rejected.

On the one hand, using this processing on images of higher resolution will lead to a better detection of small tanks in oil tank farms. On the other hand, the big oil tanks, which were easily detectable in Sentinel-2 images, tend to be missed in the circle detection step. This is due to the presence of higher frequencies and more pronounced shadows that break the circular shape of the edge segment around a tank. To overcome this issue, a low-pass filter could be applied to the image such as a Gaussian kernel. But that implies an extra parameter to set and it would blur the edges of the targeted objects.

We present a multi-scale approach. The image is scaled down by a factor  $2^{-n}$ , with  $n \in [0, 1, \dots, N]$ . Each produced image is then processed through the isoperimetric circle detection method from the smallest scale to the biggest one. At each step, overlapping detections are merged when a new circle center falls in an already detected one. This gives a more complete circle detection mask on which to apply the *a contrario* clustering method as shown in figure 3.

## 4. EXPERIMENTS

We evaluate the method on a set of oil tank farm images from Sentinel-2. This extension depends on two parameters, the number of patches from the initial method to select, and the threshold on the minimal value of local maxima in the cross-correlation map  $M$ .

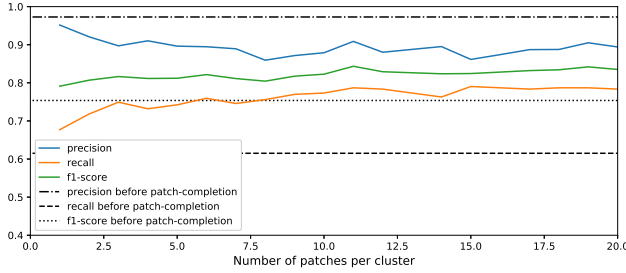


**Fig. 4:** Evolution of the precision and recall score with respect to  $m_p$ .

As illustrated in figure 4, the more reference patches are used, the better the results are. Nevertheless, there is a loss in precision, which stays around 0.9, but a high recall gain is noted. This is the expected behavior since the more patches are used, the more diverse tanks can be retrieved. We can also note that the f1-score stays quite stable with respect to this parameters but has still improved, compared to the initial method.

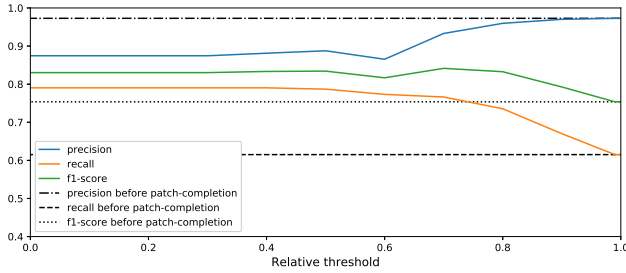


**Fig. 5:** Evolution of the precision and recall score with respect to  $\tau$ .

The performance of the model is the highest with no thresholding. The scores are held until  $\tau = 0.5$ , where one can start to notice an increase in precision and a loss in recall. When  $\tau = 1$ , the reference patch is only compared to itself, which will bring no new detection and keep the result as it was with the original method.

## 5. CONCLUSION

The proposed extension to the *a contrario* oil tank detection meets the expectation of having a higher recall, at the cost of a loss of precision. But the overall f1-score increases and the precision is still satisfying. The patch-match method introduces small false alarms, which are eliminated by the second *a contrario* clustering. We also proposed to extend the method to high-resolution images. The multi-scale approach allow the algorithm to be more versatile with the type of data that it can process and to exploit the richer information of the signal.

## 6. REFERENCES

- [1] X. Han and H. Xu, "Circular array targets detection from remote sensing images based on saliency detection," *Optical Engineering*, vol. 51, pp. 6201–, 02 2012.
- [2] X. Cai, H. Sui, R. Lv, and Z. Song, "Automatic circular oil tank detection in high-resolution optical image based on visual saliency and hough transform," in *IWECA*, 2014, pp. 408–411.
- [3] M. Jing, D. Zhao, M. Zhou, Y. Gao, Z. Jiang, and Z. Shi, "Unsupervised oil tank detection by shape-guide saliency model," *IEEE Geoscience and Remote Sensing Letters*, vol. 16, no. 3, pp. 477–481, 2019.
- [4] L. Zhang, Z. Shi, and J. Wu, "A hierarchical oil tank detector with deep surrounding features for high-resolution optical satellite imagery," *IEEE JSTARS*, vol. 8, no. 10, pp. 4895–4909, Oct 2015.
- [5] R. Soundrapandiyan, "Enhancement of an algorithm for oil tank detection in satellite images," *IJIES*, vol. 10, pp. 218–225, 05 2017.
- [6] M. Zalpour, G. Akbarizadeh, and N. Alaei-Sheini, "A new approach for oil tank detection using deep learning features with control false alarm rate in high-resolution satellite imagery," *IJRS*, pp. 1–24, 11 2019.
- [7] A. Tadros, S. Douyer, R. Grompone von Gioi, and L. Carvalho, "Oil tank detection in satellite images via a *contrario* clustering," *IGARSS*, 2020.
- [8] R. Grompone von Gioi and V. Pătrăucean, "A *contrario* patch matching, with an application to keypoint matches validation," in *ICIP*, 2015, pp. 946–950.
- [9] F. Devernay, "A non-maxima suppression method for edge detection with sub-pixel accuracy," *INRIA Research Report*, vol. 2724, 11 1995.
- [10] A. Desolneux, L. Moisan, and J. M. Morel, *From Gestalt Theory to Image Analysis: A Probabilistic Approach*, vol. 34, 01 2008.
- [11] J.P. Lewis, "Fast normalized cross-correlation," *Ind. Light Magic*, vol. 10, 10 2001.